Assessment of Delamination in Tensylon® UHMWPE Composites by Laser-induced Shock

Cristina Luminita, M. Arrigoni, Lorena Deleanu, Marcel Istrate

Assessment of Delamination in Tensylon® UHMWPE Composites by Laser-induced Shock

LUMINITA CRISTINA ALIL[1], MICHEL ARRIGONI[2]*, LORENA DELEANU[3], MARCEL ISTRATE[4]

[1]Military Technical Academy Ferdinand I, Doctoral School Engineering of Systems for Defense and Security, 39-49 George Cosbuc Av., 050141, Bucharest, Romania

[2]ENSTA Bretagne, IRDL FRE CNRS n°3744, 2 rue Francois Verny, 29806 Brest, France

[3]Dunarea de Jos University of Galai (UGAL), 47, Strada Domneasca, Galati, Romania

[4]STIMPEX SA, 46-48 Nicolae Teclu, 032368, Bucharest, Romania

Ultra-High Molecular Weight Polyethylene (UHMWPE) composites are the result of recent developments in material research for ballistic protection due to their ability to absorb the kinetic energy of the bullet by various mechanisms of dissipation, among which an important one is delamination. In order to study this mechanism independently, the laser induced shock wave testing procedure has been used on thin Tensylon® laminate samples. Laser-induced shock represents a modern approach that can be used for assessing the interlaminar bond strength between two plies of a composite material, in dynamic conditions, at high strain rates representative for a ballistic impact. Through this technique, a delamination failure stress threshold can be determined. In the present work, the laser induced shock technique was applied on the commercial UHMWPE material called Tensylon®. The delamination threshold of this material was determined by using the Novikov approach, and, compared to the literature, the results match the values determined by other means of measurement.

Keywords : delamination stress threshold, laser-induced shock wave, ballistic protection, polymer composites, Tensylon®

The industry of ballistic protection is focused on developing lightweight solutions for their strategic use. First, light weight armors increase the autonomy of vehicles in battlefields by reducing the fuel consumption determined by the weight penalty of metal shielding materials. At the same time, they offer to enhance the level of personal protection and increase the mobility of the users. Ultra-High Molecular Weight Polyethylene (UHMWPE) - based composite assemblies have been identified as some of the most relevant solutions for light weight armors. The hard (hot-pressed) ballistic laminates available under the tradename of Tensylon® (manufactured by DuPont®, USA) are UHMWPE-based materials that could fulfill requirements related to ballistic protection.

Delamination (i. e. interlaminar fracture toughness) is a phenomenon specific to laminates. Figure 1 illustrates the delamination associated phenomena on a 50 cm x 50 cm Tensylon® hard panel, consisting of 196 layers (initially approximately 23 mm thick), impacted by five 7.62*39 mm Full Metal Jacketed, Lead Core (FMJ-LC) bullets from a distance of 10 m, at ~700 m/s. The plate has been sandwiched, before being hit, between two thick steel plates (2.5 mm). The back and forth travel of the shock wave, enhanced and prolonged by the presence of the steel sheets, determined a massive delamination throughout the volume of the panel.

Delamination is, among processes as fiber melting, bulging (which could produce curling or buckling of the failed filaments/layers) and stretching (which leads to back face deformation), one of the physical mechanisms of UHMWPE-based and other composite materials for dissipating the kinetic energy during shock and impact events. However, in modelling approaches, delamination is often neglected, as it is considered to have small influence on other characteristics of interest, such as fiber strength or ply stiffness [1-2].

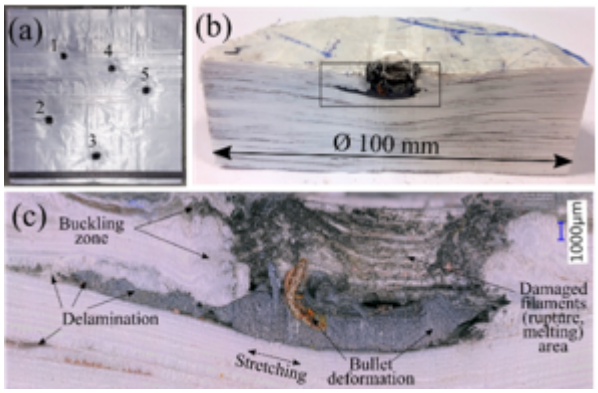

Fig. 1. (a) Tensylon® plate impacted by five 7.62*39 mm FMJ-LC bullets; (b) section through the impact zone in the plate, via waterjet-cutting; (c) detailed view of the impact zone, obtained with a Keyence VHX-5000 digital microscope, showing the UHMWPE mechanisms of stopping the bullet penetration

Nevertheless, delamination is considered to be a key mechanism in the material response, as a sign of softening [3], which subsequently is reported to actually enhance the ballistic resistance of laminates [4-6]. Therefore, it is useful to know more about the dissipative role played by the delamination process in the prospect of enhancing the performance of composite-based light weight armor.

The laser induced shock wave technique, at the base of the laser adhesion test (LASAT) [7] is a modern approach especially used in studying the adhesive bonding of light-weight, multilayered composites and adhesively bonded assemblies used in the aeronautic and naval structures. Its ability in establishing the performance of multilayered materials under dynamic loadings, at a local scale, is highlighted in numerous articles and thesis [7-9].

The work presented in this paper is an experimental approach conducted on Tensylon® laminate, a material

* email: michel.arrigoni@ensta-bretagne.fr

which has not been extensively studied at mechanical level, to the authors' knowledge, in spite of its acknowledged ballistic performances. This paper presents some of the results obtained by testing 1.25 and 2.45 mm thick Tensylon® laminate samples subjected to the laser induced shock wave technique.

The article is organized as follows. After the introduction, section two provides a brief description of the manufacturing process of the Tensylon® composite materials involved in this study. Section three contains the layout of the experimental procedure of laser induced shock wave technique and the description of the used equipment. Section four presents test results in terms of time resolved free surface velocity (FSV) diagrams. Section five expands the approach for assessing the failure stress threshold of the studied UHMWPE materials. The last section is dedicated to general conclusions and future prospects.

Experimental part

Description of the materials

Tensylon® is a representative material for the highly oriented polyethylene tapes, obtained through an industrial procedure, called solid state extrusion. Unlike Dyneema® and other types of fibrous UHMWPE worldwidely used for a variety of purposes, the oriented filaments are difficult to be characterized individually and the matrix constituent cannot be easily replaced in order to study its influence on the overall composite performance, as it represents a different phase of the same polyethylene material [10]. However, the authors are mainly interested in the ballistic proficiency of these materials, apart from any other use and, from this point of view, Tensylon® is an affordable solution that exhibits similar performance to the most ballistic-efficient versions of fiber-based UHMWPE composites [11].

Currently, there is only one type of Tensylon® tape commercially available under the name Tensylon® HSBD 30A, which is manufactured in the shape of a 1.60 m wide double-layered bi-directional criss-cross tape, having a total length of approximately 300 m [12]. Tensylon® laminates can be obtained by pressing several cut-to-size layers, at 15.2 MPa and 120°C maximum temperature. Its internal structure is similar to other UHMWPE-based products, such as Dyneema® HB26 or HB50, which are $[0°, 90°]_n$ sequences, i.e. a criss-cross pattern. Each layer consists in unidirectionally oriented filaments and about 20% adhesive matrix (percentage characteristic to all oriented UHMWPE materials, either fiber or filament-based) [13]. Figure 2 depicts microscopical cross sections, obtained by water jet cuttting from Tensylon® laminate samples, revealing its layered structure composed of a succession of plies of about 57 µm in thickness. In order to obtain a more detailed microscopic observation, polishing with very fine particles sized down to 40 nm is required [14].

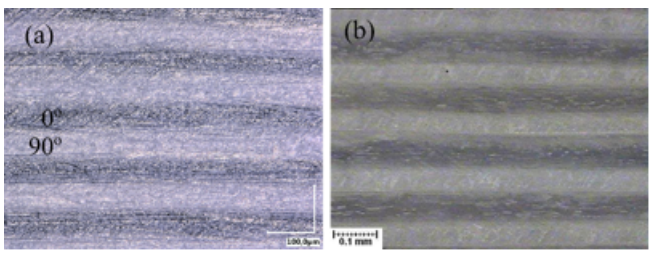

Fig. 2. Microscopic observations of polished Tensylon® laminate, using (a) 5µm grit silicon carbide paper and (b) 0.6 µm alumina polishing suspension on felt. One ply is approximately 57 µm thick

The Tensylon® laminate samples (having the internal structure depicted in fig. 2) have been obtained by water jet cutting of small pieces (10 mm x 20 mm) from 25 cm x 30 cm rigid plates, specially hot-pressed for these tests, having a thicknesses of 1.15±0.05 mm (obtained by pressing together 20 layers) and 2.45±0.05 mm (obtained by pressing together 40 layers) (fig. 3).

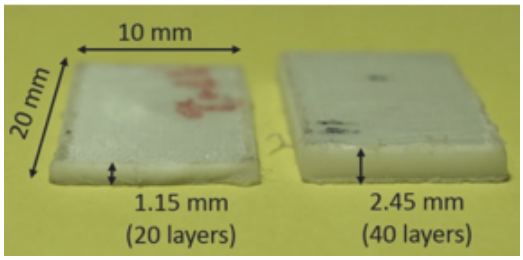

Fig. 3. Tensylon® laminate samples dimensions

Description of the setup

Testing procedure

During the irradiation, a thin layer (submicronic) of material is sublimated in plasma (fig. 4) in a very short time (< ns, similar to a detonation). The plasma expansion pushes into the sample, resulting in a shock wave (figure 4-b). When a layer of water or another transparent material is added at the place of irradiation (fig. 4-c), it plays a confinement role as it retains the plasma expansion. It results in an increase by a factor of 3 of the generated pressure and by a factor of 3 to 5 of the duration of the pressure pulse (fig. 4-a).

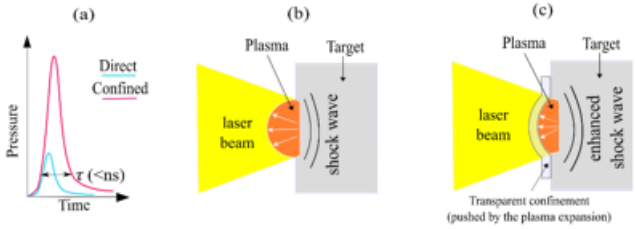

Fig. 4. a. Schematic view of the laser-induced pressure (direct/confined) in time; b. Laser-matter interaction and generation of the shock wave within the target; b. Confined laser-matter interaction

The general condition of achieving a laser induced shock wave is that the power density (ϕ) should be of the order of GW/cm^2, but it must remain below 4 GW/cm^2 in air and 8 GW/cm^2 in water, in order to avoid breakdown at ambient conditions in front of the sample. This condition sets the maximal laser spot size at impact, in air and under water. The density of power is calculated with relation (1):

$$\phi = \frac{E_{max}}{\tau S} \leq 4\ GW/cm^2, \quad (1)$$

where E_{max} is the maximum energy provided by the laser source, τ is the duration of the laser-induced pressure and S is the laser spot size on the sample. This relation between the power density and the induced peak pressure in water confined regime was determined empirically by Berthe and Sollier [15-16], based on the graph depicted in figure 5.

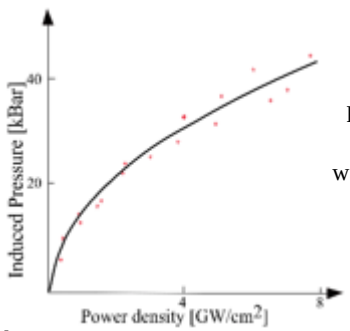

Fig. 5. Maximal pressure induced by laser shock wave versus power density in a target [15-16]

Equipment and setup

In these experiments, the shock was created by the laser-matter interaction in water confined geometry [15-16]. This configuration requires focusing the laser beam on one face of the sample, in such way that its propagation is normal to the sample thickness (out-of-plane direction) (fig. 6).

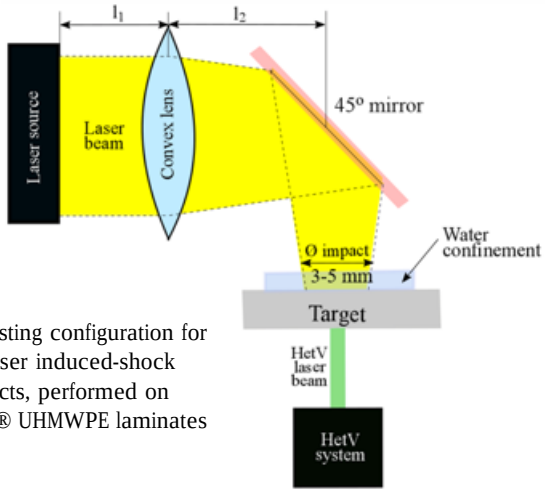

Fig. 6. Testing configuration for the laser induced-shock impacts, performed on Tensylon® UHMWPE laminates

The laser source used was a Quanta-Ray® Pro-350-10 that could provide a maximum measured energy of 2 J at a wavelength of 532 nm and 3.9 J at 1064 nm, with a Gaussian like pulse of 9 ns of duration at half maximum. The incident energy per shot was measured with a Gentec® Maestro® Joulemeter containing an attenuator protection. The laser pulse duration was measured with an Alphalas® fast response photodiode and a 40 GS/s Agilent oscilloscope. Both pulse duration and energy have been regularly checked along the experimental session and the measured parameter resulted in a less than 2 % variability.

As the laser-matter interaction also depends on the irradiated material, it has been chosen to add a sacrificial layer of a 16 µm thick of aluminum foil on the shocked face, considering that the pressure dependence on the density of power is known for aluminum [15-17]. This aluminum layer was stuck on the Tensylon® sample with acacia honey and strongly pressed by hand. The total thickness of the sample is then measured and, by deduction, the honey thickness is estimated to be 10 ±5 µm. Acacia honey is a material of interest, well known by acousticians since it results in a good acoustic coupling between materials, by avoiding the presence of bubbles.

In laser induced shock experiments, one of the most accessible physical parameters is the free surface velocity, obtained by the use of contactless methods like laser Doppler interferometry, which is fast enough for observing such rapid phenomenon. In order to measure the time resolved particle velocity on the free surface of the UHMWPE samples, Heterodyne Velocimetry (HetV in English), also called Photonic Doppler Velocimetry (PDV in U.S.A.) equipment manufactured by IDIL® [18], has been installed in such way that it measured the free surface velocity on the opposite face of the laser irradiation, coaxially with the irradiation spot (fig. 6). This requires aligning the laser probe of the HetV with the incident laser beam. The used HetV equipment has an operating wavelength of 1550 nm (invisible) and a diameter of the laser beam of 150 µm. Basically, the HetV system will measure the light phase shift (Doppler shift) between a reference beam and the collected light reflected from the free surface of the sample. The collected signal is under the form of a sinusoid response with a modulated period that is a function of the Doppler shift, i.e. the velocity of the sensed material.

HetV signals have been processed with *Cafeine®* software [18] that performs a step by step Short Time Fourrier Transform (STFT) with a temporal window of 800 samples (20 ns width) and 1 sample of overlapping (0.025 ns). It gives a time resolved velocity under the form of spectrograms, with a ΔV . $\Delta T \geq 1E^{-7}$ accuracy, if velocity is stable, and ±10 m/s accuracy, if velocity is unstable. The data extraction lead to the time resolved FSVs that were unfortunately sensitive to the selected region of interest of the spectrogram and the STFT. In order to avoid averaging that may be detrimental to the accuracy of data extraction, additional care has been taken by choosing the region of interest using a polygonal selection of the most intense parts of the spectrogram.

In order to tune the density of power (i.e. the pressure peak), distance l_2 (fig. 6) has been changed several times, aiming to obtain a higher energy density by changing the laser spot size, which has been checked using a photosensitive paper. It was also possible to modify the laser energy to get two different densities of power for a similar laser spot size.

The velocity record was triggered on the laser source firing event. The laser beam took, therefore, about 3 ns to reach the target. In order to estimate the time taken by the laser-matter interaction and the acquisition chain delay time response (electronic devices + coaxial cables), strikes haves been performed on pure aluminum sample. From HetV measurements, the longitudinal sound velocity on aluminum could then be calculated by knowing the aluminum thickness and the time between waves back and forth in the sample. It is estimated to be 6400 m/s ± 50 m/s. By measuring the first transit time, a correction delay is fixed in order to get the correct longitudinal velocity for low amplitude shock waves in order to reduce the damping effect on the transit time. This process has been repeated 9 times, yielding to an average delay time of 110 ns with 3 ns of standard deviation. The speed of sound in honey at ambient temperature of 20°C is about 2030 m/s [24]. The estimated time taken by the shock to transit the 16 µm Al layer and 10 µm honey is, then, of the order of 8 ns. This time delay is the time to be added to the zero time of the trigger to obtain the instant of the shock generation on the sample (the authors consider the laser matter interaction that creates the shock is less than 1 ns).

Method for interpreting the results

The mechanism of the laser-induced delamination in multilayered composites is illustrated in figure 7. It represents the basis for the interpretation of the results obtained in the present work.

In such laminates, the laser-induced shock wave travels through the whole composite thickness, along with a release wave that follows after the loading ends, reaching, one after the other, the back face. After the shock wave is reflected as release waves at the free surface, these release waves will cross the release waves of the unloading, coming from the front face. This situation marks the place of a dynamic tensile strength known for provoking spall fracture [19]. In case of non-spalling (travel between t_1 and t_3 in space-time diagram and dashed line in velocity-time diagram on fig. 7), it means the induced stresses were lower than the failure stress and, so, the shock wave travels back and forth in the whole target thickness several times.

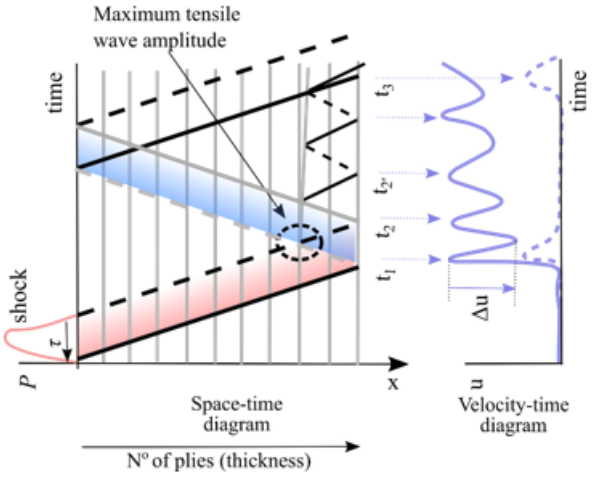

Fig. 7. (a) Schematic 1D Time/position diagram - the shock (compression) is represented in solid full line, the release (tension) in dashed lines; (b) Associated back face velocity versus time schematic graph; dashed line – no spallation, full line- spallation

Delamination or spalling (fig. 7, marked by instants t1, t2, t2' on the space-time diagram and by full line in velocity-time diagram) means that the shock surpassed the strength of the material. Voids are created inside the material, adding an inner free surface that will affect wave propagation.

It is understood that what is called *spall* or *delamination strength* is loading- and sample-dependent [19]. In the proposed approach, it means the ability to resist the tensile load consecutive to the laser induced shock wave in the sample of interest, taking into account its material and thickness aspects. Spallation process is actually initiated by a tensile state provoked by the occurrence of release waves that propagate in opposite directions: one coming from the shock reflection at the free surface, the other from the unloading at the impacted face. Ideally, according to [20], the transition from non-spalling to spalling behavior of a bonded assembly occurs when the free surface velocity - time diagram changes (schematically) as presented on figure 8. It illustrates the velocity signals obtained in a homogenous medium for pressures slightly above and below the damage threshold. The peak free-surface velocity, u_0, and the free-surface velocity just before the arrival of the spall pulse, u_m, are determined directly from the free-surface velocity profile. In order to evaluate the dynamic tensile strength σ_{spall}, the following linear approximation ([19-20]) is extended to our composite materials, as considered in previous studies [9]:

$$\sigma_{spall} = \frac{1}{2}\rho_0 c_0 \Delta u \qquad (2)$$

where $\Delta u = u_0 - u_m$ is the so-called *velocity pullback* (the velocity gap measured between the top of the first velocity peak and the take-off point). In some cases, as in the case of CFRPs studied in [9], an extra small acceleration after the first velocity peak may appear and this will be ignored, as it is induced by a wave reflection in the outer epoxy layer.

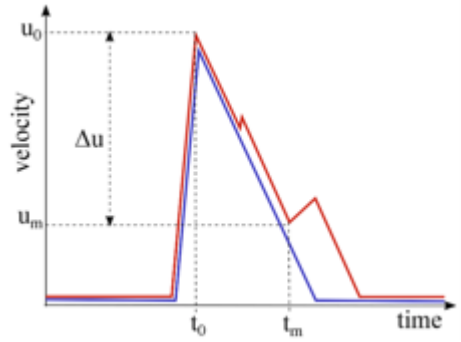

Fig. 8. Schematic representation of velocity signals of the back (free) surface. The red (upper line) and blue represent, respectively, a signal slightly above and below damage threshold. The blue signal has been normalized to the red signal maximum

Results and discussions

A series of Tensylon® samples, numbered from T-1 to T-10, have been impacted by the laser beam, at various densities of power. The samples did not only suffer inside delamination phenomena, but were also affected on the outside. As a consequence, after each strike, the authors could immediately observe one major consequence on the stricken face: the aluminum foil has been destroyed, approximately marking the diameter of the size of the laser beam due to the laser-matter interaction - figure 9(a). Another feature exhibited by the samples whose spall strength was initiated by the laser power is the appearance of a small bulge on the free surface, similar to the deflection exhibited by a thicker protection panel in the case of ballistic impact. This represents a sign of internal changes (such as delamination, spallation, elongation or a combination of them), (fig. 9(b) and 9(c)).

Strikes on samples T-7 and T-8 were too week to allow for the HetV system recording with a suitable signal to noise ratio. Therefore, the authors were not able to extract velocity signals from the corresponding spectrograms. For all the other strikes, the experimental data is gathered in table 1, in the appendix.

It should be noted, as a remark, that the extractions of time resolved velocities have been done with difficulty because of the semi-transparency of Tensylon® UHMWPE to the 1550 nm wavelength of the HetV laser, illustrated in figure 10, on the example of sample T-9 spectrogram.

Indeed, on figure 10, at least three rising fronts, delayed of 33 ns, can be observed. The first rising front indicated in the figure is very subtle; the second rising front reaches a velocity signal at half amplitude of the highest observable peak, corresponding to the third rising front. Considering the longitudinal velocity in the sample, the authors suspect a pre-existing crack or porosity at 76±5μm from the free surface. This explanation matches with the fact that the material velocity inside the sample is half the one of the free surface. Since the highest peak of velocity is obtained for the third rising front, the authors kept this last as being the shock breakout at the free surface.

By further analyzing the spectrogram in figure 10, it could be obtained the speed of sound for the Tensylon® laminate material. A sharp rising edge can be observed at around 0.615 ± 0.005 μs. It indicates the breakout of the laser induced shock wave at the free surface and corresponds

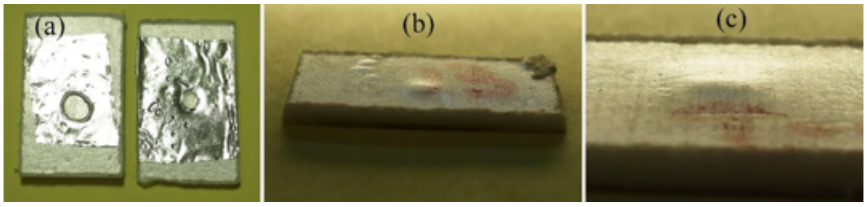

Fig. 9. Post-mortem appearance of the samples (a) strike face; (b) and (c) back face deflections (illustrated for samples T-9 and T-10, respectively)

Sample	Thickness [mm]	Energy [J]	Power Density [GW/cm²]	Observable peaks		Observations
				V_i [m/s]	t_i [µs]	
T-1	1.15	1.16	1.18	86	0.63	**Figure 12** Focal spot 3.7 mm V_{max}=142 m/s [t=1.18 µs] **Spalled**
T-2	1.15	1.16	1.18	143	0.66	**Figure 13** Focal spot 3.7 mm V_{max}=145m/s [t=0.66 µs] **Spalled**
T-3	1.15	1.16	1.18	125	0.60	**Figure 14** Focal spot 3.7 mm V_{max}=161m/s [t=0.69 µs] **Spalled**
T-4	1.15	0.34	0.64	46	0.79	**Figure 15** Focal spot 3.7 mm V_{max}=67 m/s [t=1.06 µs] **Not spalled**
T-5	2.45	1.16	1.18	85	1.81	**Figure 16** Focal spot 3.7 mm V_{max}=101 m/s [t=1.83 µs] **Spalled**
T-6	2.45	0.63	0.64	23.7	1.7	**Figure 17** Focal spot 3.7 mm V_{max}=28 m/s [t=1.69 µs] **Not spalled**
T-9	1.15	*1.16*	1.80	267	0.56	**Figure 9** Focal spot 3 mm V_{max}=267m/s [t=0.55µs] **Spalled**
T-10	1.15	*0.46*	0.71	228	0.55	**Figure 18** Focal spot 3 mm V_{max}=228 m/s [t=0.55µs] **Spalled**

* Symbols: V_i – first peak of the free surface velocity on the HetV spectrogram; t_i = time travel of the shock wave from the impact surface to free surface

Table 1
RESULTS OF LASER SHOCK TESTING ON UHMWPE TENSYLON® SAMPLES*

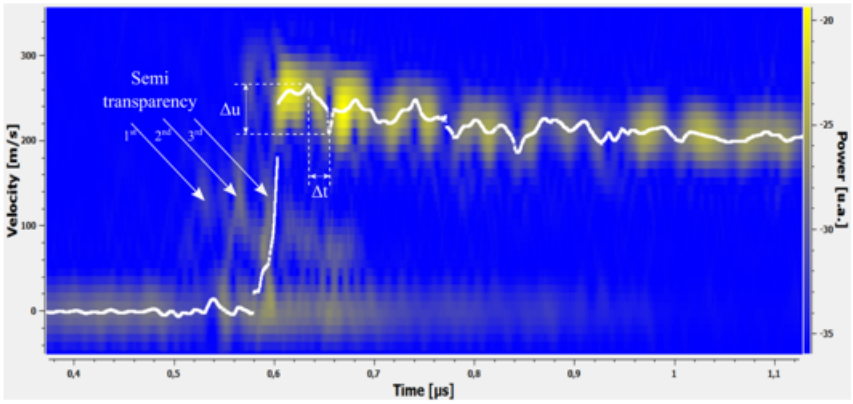

Fig. 10. Spectrogram of the free surface velocity, sample T-9 (thickness 1.15 ±0.01 mm, density of power 1.80 GW/cm²)

to an average shock velocity of 2300 ± 50 m/s. Extracted velocity data gives a peak velocity of 267 m/s at 0.615 µs. A valley is noted at 0.654 µs, with a velocity dropping down to 210 m/s. The material velocity behind the shock front within the material is half of the free surface velocity, so, about 135 m/s. Next the relation (3) between shock velocity U_s and material velocity U_p is used:

$$U_S = C_0 + s \cdot U_p \quad (3)$$

with s = 3.73, the coefficient given by Lässig [23] for Dyneema®. By assuming the same s value for Tensylon®, it leads to C_0=1797 ± 50 m/s, close to the value of 1898 m/s, given by Lässig for 980 kg/m³ Dyneema® [22]. By considering formula (4) as an estimation of the strain rate during delamination:

$$\dot{\varepsilon} = -\frac{1}{2C_0}\frac{\Delta u}{\Delta t} \quad (4)$$

the strain rate is estimated at about 2.21e^6 s^{-1}, a maximum during the process of delamination.

In figure 11, the authors have superposed the recorded velocities for several samples (using spectrograms in figures 12 to 18 from, in the appendix), at different power densities, in order to compare their shapes. Analyzing the spectrograms, one may notice different amplitudes of the free surface velocities, for a range of power densities (0.64-1.80 GW/cm²). As expected, the transit time of the shock wave is smaller in thinner samples. Highest velocities are obtained on samples T-9 and T-10 (1.15 mm thick), respectively, for 1.80 and 0.71 GW/cm². The arrival time is nearly the same in both cases (around 0.6 µs), which means a transit velocity of about 2300 m/s, available as well for samples T-1, T-2 and T-3. For sample T-4, the density of power is significantly lower than for previous ones. In the case of samples T-5 and T-6, their spectrograms are obtained at power densities of 1.18 and 0.64 GW/cm², respectively. Both samples T-5 and T-6 are

Sample	Thickness [mm]	ΔU [m/s]	Δt [s]	σ_{rupt} [MPa]	$\dot{\varepsilon}$ [s^{-1}]
T-1	1.15	46.3	93.7	58	-3.65E+06
T-2	1.15	40.2	124	48	-1.97E+06
T-3	1.15	60	120	58	-8.74E+06
T-5	2.45	18	80.8	32	-1.37E+06
T-9	1.15	57	210	46	-2.21E+06
T-10	1.15	80	185	33	-2.34E+06
Mean rupture stress				45.8	

*ρ=0.94 g/cm^3 and C_0=1797 m/s

Table 2
NOVIKOV APPROACH IN TENSYLON® SAMPLES*

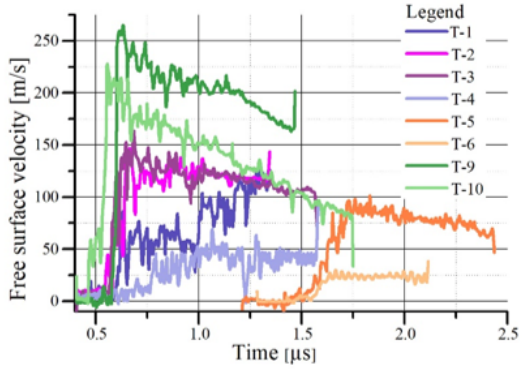

Fig. 11. Free surface velocities extracted from spectrograms recorded with the HetV system, according to experimental conditions specified on table 1, appendix

2.45 mm thick, thus, the shock propagation is longer and the break out at the free surface occurs in about 1.7 μs. Shots on samples T-4 and T-6, however, did not yield to a visible bulging at the free surface. Likewise, their free surface velocity signals do not exhibit a clear fall after the shock break out at free surface, as it is the case for other strikes. Thus, the authors consider that these shots did not spall the sample (there is no delamination), without more convincing diagnostics.

Spectrograms of T-9 and T-10 samples have some oscillations appearing around the peak, which is an evident sign of delamination for the reasons explained in figure 8. In addition, samples T-9 and T-10, as well as samples T-1, T-2, and T-3, show a bulged free surface and a clear velocity fall after the shock break out on spectrograms. The authors considered these samples as spall (delaminated).

Spall strength assessment for Tensylon®

Considering the shapes of the FSV signals, the Novikov [20] approach was eligible for spectrograms of shots on samples T-1, T-2, T-3, T-5, T-9 and T-10. The Novikov equation (2) indicates the maximum tensile stress at rupture. In this formula, Δu (also referred to as *pullback velocity)* is the first velocity drop or the difference between the maximum amplitude and that of rebound, as illustrated in figures 7 and indicated in figure 10. The sound velocity considered in the calculations was the one determined earlier, C_0=1797 m/s. The resulted stress and strain rate at delamination were gathered on table 2, in the appendix.

There is a certain uncertainty about the spall strength determination in Tensylon® composites by the Novikov approach. This strength is ranging from 32 MPa to 58 MPa. These discrepancies can be explained by the fact that the interfacial debonding depends on the local crack initiation and crack propagation energies. It is known that composite materials have some defects, such as porosity and preexisting cracks that may affect the amount of energy required for initiating and propagating cracks. Thus, the obtained values appear reasonable, as it is known from the literature that UHMWPE matrix is very weak and shear stresses could be lower than 10 MPa for Dyneema® laminates under quasi static loadings, according to O'Masta [21], and around 50 MPa under high strain rate loadings in tensile model, according to Lassig et al. [6]. The fact that the delamination stress at high strain rate is higher than that in quasi static situation is also reported by Ecault [8] and Gay [9] for composite materials and in [19] for metallic ductile materials.

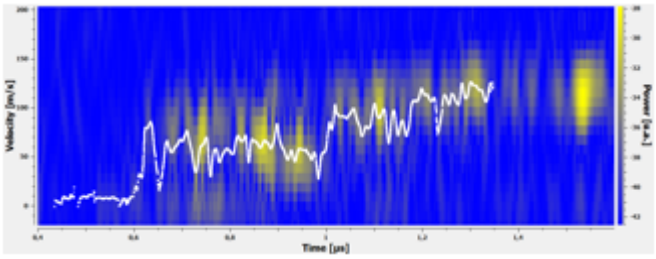

Fig. 12. Spectrogram of Sample T-1

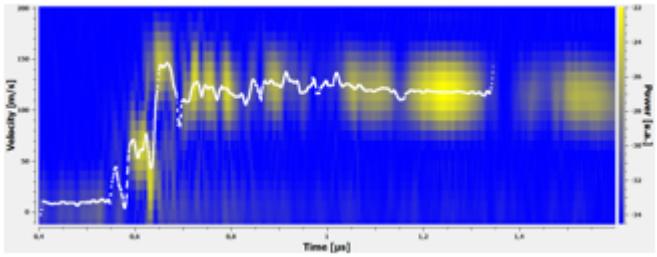

Fig. 13. Spectrogram of Sample T-2

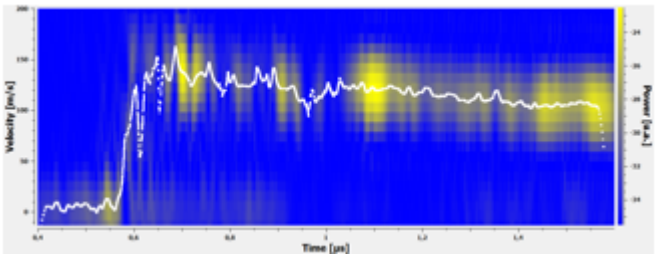

Fig. 14. Spectrogram of Sample T-3

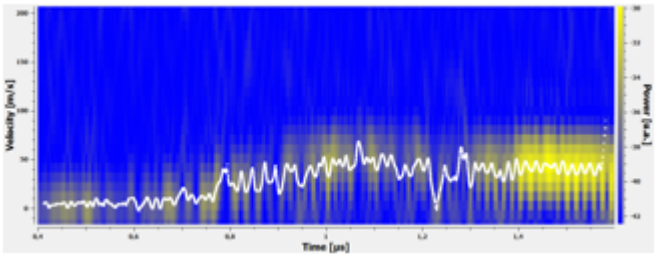

Fig. 15. Spectrogram of Sample T-4

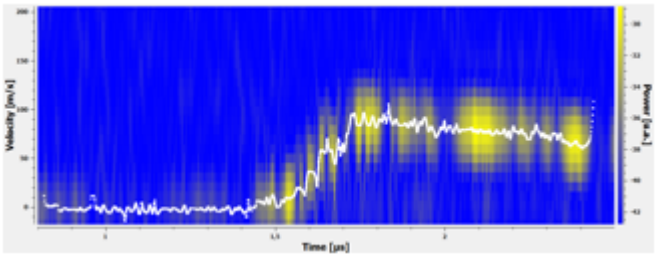

Fig. 16. Spectrogram of Sample T-5

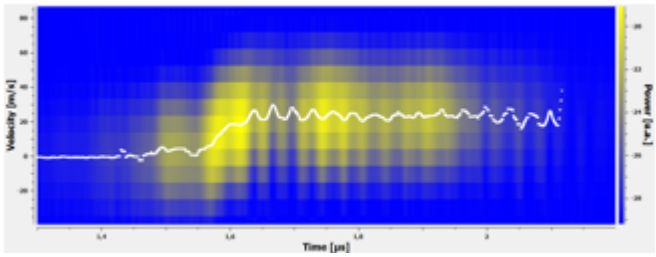

Fig.17. Spectrogram of Sample T-6

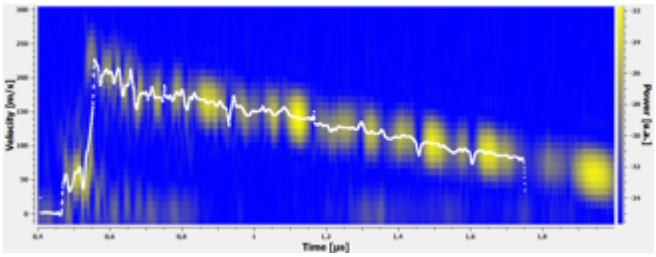

Fig. 18. Spectrogram of shot no 6 /Sample T-10

Conclusions and future prospects

Laser induced shock definitely represents a technique to be taken into account in order to study the delamination mechanism of UHMWPE composite materials used in ballistic protection since it provides high strain rates, representative for a ballistic impact situation. This technique is also appreciated for its local aspect of strength assessment.

These tests represent the first attempt in evaluating the delamination phenomena of UHMWPE materials by laser induced shock wave, i.e. under very high strain rates (>1e6 s^{-1}).

The spall strength estimated is, of course, dependent on the strain rate, but the order of magnitude is close to that obtained on other types of UHMWPE composites, such as Dyneema®.

Overall, the results prove that the studied UHMWPE composites (Tensylon® brand) are materials with a certain amount of internal defects, roughness and wavy effects that vary locally throughout the thickness, a fact that, subsequently, significantly affects their performance at both quasi-static and dynamic tests.

Further investigation using tools such as micro-tomography is advisory. For future experiments, more care will be taken concerning the transparency of the material to the 1550 nm wavelength of the HetV system. A thin metal coating obtained by vapor deposition could help remedy this aspect.

Numerical simulation could also help understanding the shock propagation and the spall process, particularly for the stress estimation by an inverse approach. An effort will be done on this direction in the future.

ACKNOWLEDGMENTS: The authors acknowledge the ERASMUS+ program of the European Commission, which facilitated an internship for Luminia-Cristina Alil at ENSTA Bretagne, during her PhD studies, between september 2015 and march 2016. The authors are also grateful for the help received from Thomas Bonnemains (IUT Brest), who prepared the cut-to-size samples used in these tests, via waterjet cutting.

References

1. NAVARRO C., Simplified modelling of the ballistic behaviour of fabrics and fibre reinforced polymeric matrix composites, Key Engineering Materials, p. 141–143:383–400, 1998, https://doi.org/10.4028/www.scientific.net/KEM.141-143.383

2.YONG M., IANNUCCI L., FALZON B. G.,Efficient modelling and optimisation of hybrid multilayered plates subject to ballistic impact, International Journal of Impact Engineering, 37(6), p. 605-624, 2010, https://doi.org/10.1016/j.ijimpeng.2009.07.004

3.WISNIEWSKI A., AND PACEK D. - Experimental research and numerical analysis of 9 mm Parabellum projectile penetration of ultra-high molecular weight polyethylene layers, Problemy Techniki Uzbrojenia, 42(127), p. 55-64, 2013

4.MORII T., HAMADA H., HIROYUKI D., DESAEGER M., GOTOH A., YOKOYAMA A., VERPOEST I., MAEKAWA Z., Damage tolerance of glass mat/epoxy laminates hybridized with flexible resin under static and impact loading, Composite structures, vol. 32 (1-4), p. 133–139, 1995, https://doi.org/10.1016/0263-8223(95)00082-8

5.KANG T.J., KIM C., Energy-absorption mechanisms in Kevlar multiaxial warp-knit fabric composites under impact loading, Compos. Sci. Technol., vol. 60 (5), p. 773–784, 2000, https://doi.org/10.1016/S0266-3538(99)00185-2

6.LASSIG, T., BAGUSAT, F., PFANDLER, S., GULDE, M., HEUNOSKE, D., OSTERHOLZ, J., ... & MAY, M. (2017). Investigations on the spall and delamination behavior of UHMWPE composites. Composite Structures, 182, 590-597, https://doi.org/10.1016/j.compstruct.2017.09.031

7.BERTHE, L., ARRIGONI, M., BOUSTIE, M., CUQ-LELANDAIS, J. P., BROUSSILLOU, C., FABRE, G., ... & NIVARD, M. - State-of-the-art laser adhesion test (LASAT), Nondestructive Testing and Evaluation, 26(3-4), 303-317, 2011, https://doi.org/10.1080/10589759.2011.573550

8.ECAULT, R., BOUSTIE, M., TOUCHARD, F., PONS, F., BERTHE, L., CHOCINSKI-ARNAULT, L., ... & BOCKENHEIMER, C. (2013). A study of composite material damage induced by laser shock waves. Composites Part A: Applied Science and Manufacturing, 53, 54-64, https://doi.org/10.1016/j.compositesa.2013.05.015

9.GAY, E., BERTHE, L., BOUSTIE, M., ARRIGONI, M., & TROMBINI, M. - Study of the response of CFRP composite laminates to a laser-induced shock, Composites Part B: Engineering, 64, p. 108-115, 2014, https://doi.org/10.1016/j.compositesb.2014.04.004

10.HEARLE, JOHN WS (ed.). High-performance fibres. Elsevier, 2001.

11.X. CHEN, Y. CHU - Failure mechanisms and engineering of ballistic materials. In: Chen, X.(Ed.), Advanced Fibrous Composite Materials for Ballistic Protection,Woodhead, 2016, 263-304,https://doi.org/10.1016/B978-1-78242-461-1.00009-1

12.*** Tensylon HSBD 30A - Product specification sheet, www.dupont.com, accessed december 2017

13.BHATNAGAR A, editor. Lightweight ballistic composites: military and lawenforcement applications. CRC Press; 2006

14.RUSSELL, B. P., et al. The high strain rate response of ultra high molecularweight polyethylene: from fibre to laminate.IInternational Journal of Impact Engineering 60 (2013): 1-9, https://doi.org/10.1016/j.ijimpeng.2013.03.010

15.BERTHE, L., FABBRO, R., PEYRE, P., & BARTNICKI, E. - Wavelength dependent of laser shock-wave generation in the water-confinement regime, Journal of Applied Physics, 85(11), 7552-7555, 1999, https://doi.org/10.1063/1.370553

16.SOLLIER, A.; BERTHE, L.; FABBRO, R., Numerical modeling of the transmission of breakdown plasma generated in water during laser shock processing, European Physical Journal-Applied Physics Vol.16 Issue: 2 p. 131-139, (2001), https://doi.org/10.1051/epjap:2001202

17.ARRIGONI M., MONCHALIN J.-P., BLOUIN A., KRUGER S. E., LORD M., Laser Doppler Interferometer based on a solid Fabry-Perot Etalon for measurement of surface velocity in shock experiments", Measurement Science & Technology 20, 1, (2009).
18.PRUDHOMME, G., MERCIER, P., BERTHE, L., BÉNIER, J., & FRUGIER, P. A. - Frontal and tilted PDV probes for measuring velocity history of laser-shock induced calibrated particles, Journal of Physics: Conference Series, Vol. 500, No. 14, p. 142022, IOP Publishing, 2014
19.ANTOUN, TARABAY. Spall fracture. Springer Science & Business Media, 2003.
20.NOVIKOV S.A., DIVNOV, I.I., IVANOV, A.G., The Study of Fracture of Steel, Aluminum, and Copper under Explosive Loading, Phys. Metals Metal Science (USSR), 21(4), 608–615 (1966).
21.O'MASTA, M. R., DESHPANDE, V. S., & WADLEY, H. N. G. (2015). Defect controlled transverse compressive strength of polyethylene fiber laminates. International Journal of Solids and Structures, 52, 130-149, https://doi.org/10.1016/j.ijsolstr.2014.09.023
22.ALIL, L. C., ARRIGONI, M., BADEA, S. M., BARBU, C., ISTRATE, M., & MOSTOVYKH, P. S. (2017). On the Constitutive Law for the Mechanical Quasi-static Response of Criss-Cross Composites (on the Example of UHMWPE). Human Factors and Mechanical Engineering for Defense and Safety, 1(1), 4, https://doi.org/10.1007/s41314-017-0006-5
23.LASSIG, T., BAGUSAT, F., MAY, M., & HIERMAIER, S. (2015). Analysis of the shock response of UHMWPE composites using the inverse planar plate impact test and the shock reverberation technique. International Journal of Impact Engineering, 86, 240-248, https://doi.org/10.1016/j.ijimpeng.2015.08.010
24. ***Technique tables. Acoustic properties of, http://www.signal-processing.com/table.php, accessed december 2017

Manuscript received: 15.06.2018